



Original article

Antibacterial and antibiofilm effects of silver nanoparticles against the uropathogen *Escherichia coli* U12Eman Selem^a, Asmaa F. Mekky^{a,*}, Wesam A. Hassanein^a, Fifi M. Reda^a, Yasser A. Selim^b^a Botany and Microbiology Department, Faculty of Science, Zagazig University, Zagazig, Egypt^b Faculty of Specific Education, Zagazig University, Zagazig, Egypt

ARTICLE INFO

Article history:

Received 1 July 2022

Revised 21 August 2022

Accepted 19 September 2022

Available online 23 September 2022

Keywords:

Silver nanoparticles

Biofilm

Adhesion

ABSTRACT

The drug-resistant bacterial strains' emergence increases day by day. This may be a result of biofilm presence, which protects bacteria from antimicrobial agents. Thus, new approaches must be used to control biofilm-related infections in healthcare settings. In such a study, biological silver nanoparticles were introduced in such a study as an anti-biofilm agent against multidrug-resistant *E. coli* U12 on urinary catheters. Seven different silver nanoparticles concentrations were tested for their antimicrobial activities. Also, anti-biofilm activities against *E. coli* U12 were tested. Using the dilution method, the silver nanoparticles concentration of 85 µg/ml was the MIC (Minimum Inhibitory Concentration) that had excellent biocompatibility and showed significant antibacterial activity against *E. coli* U12. Scanning electron microscopy (SEM) confirmed that the highest efficient dose of silver nanoparticles was 340 µg/ml at 144 h that reduced adhesion of *E. coli* U12 to the urinary catheter. *E. coli* U12 cells ruptured cell walls and cell membranes after being examined using transmission electron microscopy (TEM). Thus, biologically prepared silver nanoparticles could be used to coat medical devices since it is effective and promising to inhibit biofilm formation by impregnating urinary catheters with silver nanoparticles.

© 2022 The Authors. Published by Elsevier B.V. on behalf of King Saud University. This is an open access article under the CC BY-NC-ND license (<http://creativecommons.org/licenses/by-nc-nd/4.0/>).

1. Introduction

Nanomedicine is a relatively new trend in medicine. Metal nanoparticles have been shown to have antibacterial, antifungal, and antiviral properties. Silver nanoparticles represent the common antimicrobial agent. Due to recent technological advancements (Patra et al., 2018), silver nanoparticles have resurfaced in the medical field. Because of their low toxicity to mammalian cells and stronger antimicrobial activity, Silver nanoparticles have been used in a variety of disciplines. Silver nanoparticles are utilized for the treatment of biofilms associated with medical devices that threaten life (Bruna et al., 2021).

* Corresponding author at: Botany and Microbiology Department, Faculty of Science, Zagazig University, Zagazig 44519, Egypt.

E-mail addresses: eman.elsaid@zu.edu.eg (E. Selem), asmaa.mekky22@science.zu.edu.eg (A.F. Mekky), wesamtarek@zu.edu.eg (W.A. Hassanein), Fifireda@zu.edu.eg (F.M. Reda), yasserselim@zu.edu.eg (Y.A. Selim).

Peer review under responsibility of King Saud University.



Biofilms are formed when bacteria attach to surfaces and form structures. These biofilm formations are the bacterial natural survival strategy for invading the host (Camele et al., 2019). They are more resistant to routinely used antimicrobial treatments, making control more challenging. As a result, the infection becomes more severe (Roy et al., 2018; Shaikh et al., 2019; Muhammad et al., 2020).

Bacterial resistance to antibiotics and the potential to colonize abiotic surfaces through the formation of biofilm are major causes of medical implant-associated infections, leading to prolonged hospital stays and patient mortality. Various strategies have been adopted in medical settings to prevent biofilm-associated infections (Li et al., 2021).

Nosocomial infections also referred to as healthcare-associated infections (HAI), are infections acquired during the process of receiving health care that was not present during the time of admission (Rosenthal et al., 2012). The most prevalent nosocomial infection was catheter-associated urinary tract infection, which was caused by pathogens that developed biofilms on urinary catheters. Catheterization for a long time with urinary catheters causes biofilm development and pathogen adhesion on the catheters (Almalki and Varghese, 2020).

New bacteria may not colonize the biofilm if they are exposed to silver nanoparticles. As a result, it's critical to look for anti-biofilm molecules that can efficiently reduce and eliminate biofilms that are associated with infections (Skóra et al., 2021). We have examined whether Silver nanoparticles could prevent harmful bacteria from forming biofilms in some hospital isolates. This study's objective was to thoroughly assess the antibacterial and anti-biofilm potential of the biologically produced silver nanoparticles against *Escherichia coli*. This study provides a good strategy to control biofilm formation associated with serious diseases such as urinary tract infections.

1.1. Contributions. Our contributions to this study are as follows:

- i) In this study, silver nanoparticles were synthesized using *Aloe vera* leaf extract and evaluated for their antibacterial and antibiofilm activities against biofilms of multidrug resistant (MDR) uropathogen. Our study showed that, silver nanoparticles exhibited significant antimicrobial and anti-biofilm activities against *E. coli* U12.
- ii) Different concentrations of silver nanoparticles efficiently reduced biofilm formation of *E. coli* U12 on urinary catheter. Therefore, pre-coating urinary catheters with silver nanoparticles can be largely utilized as anti-biofilm agent in medical fields to control uropathogens biofilms formation. This work was conducted in vitro so that it may be further examined for practical application.

2. Materials and methods

2.1. Bacterial strain

A previous collection of 50 bacterial isolates from urinary catheters was done. Morphological characters, biochemical tests, and 16S rRNA gene sequencing were used to identify these isolates. These isolates were tested towards different antibiotics and were assayed for their potential to produce biofilm (Mekky et al., 2022). As a result, *E. coli* U12 with the accession number MT498270 was chosen as the most MDR uropathogen used in this investigation (Fig. S1).

2.2. Biosynthesis of silver nanoparticles

The technique reported by Tippayawat et al. (2016) was used to biosynthesize silver nanoparticles with certain modifications.

2.2.1. Plant collection

Aloe vera seeds were obtained from the Agricultural Research Center in Cairo, Egypt, and young leaves and branches were harvested from young adult trees.

2.2.2. Plant extraction

Aloe vera leaves were washed several times with double distilled water to remove debris and particles and dried in the shade at room temperature. The leaves were washed with double-distilled water and shade dried, ground into fine powder, and stored in an air-tight container in dark at room temperature for extraction. 50 g of *Aloe vera* leaf powder was mixed with 100 ml of double-distilled water in 250-ml beaker. The above mixture was heated on magnetic heating stirrer at 40 °C for 10 min. The aqueous *Aloe vera* leaf extract was then filtered using Whatman filter paper No. 1 and stored at 4 °C and used for the preparation of silver nanoparticles (Fig. S2).

3. Bio-green synthesis of silver nanoparticles

In the preparation of silver nanoparticles samples, AgNO₃ (0.17 g) was first dissolved in 100 ml of deionized water and mixed 95 ml with 5 ml of *Aloe vera* extract solution, incubated for 30 min at 60 °C. Silver nanoparticles were observed after about 30 min which was indicated by change in color of the solution from colorless to brownish yellow and red, respectively. The formation of silver nanoparticles was confirmed by UV-visible spectroscopy. The silver nanoparticles were purified by frequent centrifugation at 18,000 rpm for 25 min, washed with double-distilled water, and were redispersed in deionized water for further characterizations.

3.1. Characterization of silver nanoparticles

The silver nanoparticles were first examined utilizing the Rigol ultra-3660 UV-vis spectroscopy in the 400–450 nm region. The functional groups and other phytochemical components responsible for the reduction and stability of the produced nanoparticles were then identified using FTIR. To verify the existence of Ag and evaluate the crystallite structure and size, the powdered specimen was exposed to CuKα1-X ray diffractometer radiation with $\lambda = 1.5406 \text{ \AA}$ and operated at 30 mA and 40 kV with 2θ (30°–140°). Sonication was done on silver nanopowder that was mixed with ethanol and placed on a copper grid, which was then dried before being inspected using TEM (JEOL-2100 HR).

3.2. Antimicrobial effect of silver nanoparticles against *E. Coli* U12

3.2.1. Dilution method

Different concentrations of silver nanoparticles were examined for their antibacterial activity towards *E. coli* U12 through the observation of the growth turbidity in liquid medium (Brain heart infusion) after incubation for 24 h at 37 °C. Then, the MIC was determined as the minimum inhibitory concentration that prevented the visual growth of *E. coli* U12 in liquid medium. Also, the minimum bactericidal concentration was detected as the lowest concentration at which there is no growth on solid media (Parvekar et al., 2020).

3.2.1.1. Colony forming units counting (CFU/ml). Different silver nanoparticles concentrations were tested for their antibacterial effect towards *E. coli* U12 using the CFU technique according to the modified Chapman et al. (2013) technique with incubation of silver nanoparticles and *E. coli* U12 for seven days.

3.3. Anti-biofilm effect of silver nanoparticles towards *E. Coli* U12

3.3.1. Congo red agar method

Brain heart infusion (37 g/L), sucrose (80 g/L), agar no.1 (10 g/L), and Congo red stain (0.8 g/L) were used to make Congo red agar medium. Congo red was prepared as a concentrated aqueous solution and autoclaved at 121 °C for 15 min, separately from the other medium constituents, and was then added when the agar had cooled to 55 °C. Different concentrations of silver nanoparticles were mixed with *E. coli* U12 (10⁵ CFU/mL) and kept at 37 °C for 48 h. Each mixture (0.1 ml) was streaked on a Congo red agar plate and kept at 37 °C for 24 h. Control consists of *E. coli* U12 suspension without silver nanoparticles. The appearance of black, dry colonies with a crystalline surface indicates biofilm formation. Weak biofilm producers usually remained pink with occasional darkening at the centres of colonies, and the appearance of pink colonies was indicated as negative biofilm bacteria. The experiment was performed in triplicate and repeated three times (Bose et al., 2009).

3.3.2. Crystal violet assay method (CV)

The pre-coating method outlined by Gudiña et al. (2010) was used in this test for assaying the anti-biofilm effect of different silver nanoparticles concentrations towards *E. coli* U12 using ELISA (Central Laboratory, Faculty of Pharmacy, Zagazig University, Egypt). Microliter plate wells were coated with different concentrations of silver nanoparticles and an *E. coli* U12 suspension (10^5 CFU/mL) was added after the wells dried. The microliter plate was maintained at 37 °C for 48 h and, by using CV, the fixed biofilm was dyed for 20 min. Control consists of *E. coli* U12 suspension without silver nanoparticles. After solubilization of the stained bounded biofilm, the Fracchia et al. (2010) equation was used to calculate the percentage of microbial adhesion:

$$\% \text{ Microbial adhesion}_c = (A_c/A_o) \times 100.$$

Where A_c is the optical density of the well with silver nanoparticles, and A_o is the optical density of the control well.

3.4. Investigation of *E. Coli* U12 biofilm production on urinary catheter following exposure to silver nanoparticles by:

3.4.1. CFU/cm² And crystal violet staining

This method was performed in vitro to inhibit biofilm development of *E. coli* U12 on urinary catheters using different concentrations of silver nanoparticles. The pre-coating method outlined by Ezeonu and Kanu (2016) with modifications was used in this test. In test tubes, the pre-coated catheter segments (3 segments for each) were incubated with *E. coli* U12 (10^5 CFU/ml) at 37 °C for seven days. After that, CFU/cm² and the degree of CV coloring on the urinary catheter were used to determine the biofilm development. Untreated catheter segments were used as a positive control.

3.4.2. Scanning electron microscopy study (SEM)

SEM confirmed *E. coli* U12 biofilm formation on the urinary catheter after treatment with silver nanoparticles according to Li et al. (2015). Urinary catheter segments were taken from the above method (CFU) for up to seven days and were processed using standard techniques. The SEM technique was performed in the Mansoura laboratory of electron microscopy, Mansoura University, Egypt. Each sample was gold coated using a gold sputter and viewed by SEM (JEOL JSM 6510 IV).

3.5. Transmission electron microscopy study (TEM)

The TEM technique was performed in the Mansoura laboratory of electron microscopy, Mansoura University, Egypt, and was carried out according to Mirzajani et al. (2011). An examination was carried out using a JEOL JEM-2100 TEM.

4. Statistical analysis

One-way ANOVA was used to analysis the data. As described by Dytham (1999), the programme SPSS, version 14 (SPSS, Richmond, USA), was used. The significance of the results was determined at $p < 0.05$ by using Duncan's multiple range test. Each result is the average of 3 replicates \pm standard error.

5. Results

5.1. Green synthesized silver nanoparticles characterization

The shift in solution color from greenish-yellow to brown during silver nanoparticles synthesis indicated the reduction of silver oxide salt (Fig. S3).

5.1.1. U.V. Spectrophotometric analysis

The characteristics of silver nanoparticles are usually apparent at wavelengths between 400 and 600 nm. The UV-vis spectra of the synthesized silver nanoparticles utilizing the aqueous extract of *Aloe vera* indicate a blue shift of the absorption band as the concentration of AgNO_3 increases. The absorption peak for 1 mM, 2 mM, 3 mM, 4 mM, and 5 mM specimens is located between 400 and 450 nm (Fig. S4). According to the results, silver nanoparticles were produced in the extract where the Ag^+ was reduced to Ag^0 .

5.1.2. FTIR Spectroscopic analysis

The FTIR spectra of the synthesized silver nanoparticles using the green technique illustrated a peak at 442 cm^{-1} that corresponds to hexagonal Ag symmetric bending vibrations. In addition, a peak at 878 cm^{-1} owing to the weak vibration of Ag (Fig. 1).

5.1.3. XRD analysis

As shown in Fig. 2, the X-ray diffraction pattern of the produced silver nanoparticles was taken. All of the sample's diffraction peaks demonstrated that the silver nanocrystalline production was pure and the same as the hexagonal phase with Wurtzite structures.

5.1.4. HR-TEM analysis

By TEM examination, the crystalline properties and size of the produced nanoparticles can be estimated. Fig. 3 demonstrates photos at various magnifications (50 and 100 nm) taken with the JEOL-2100. TEM photographs exhibit particle sizes ranging from 9.26 to 31.18 nm. Otherwise, it confirmed the hexagonal structure of the synthesized silver nanoparticles.

5.2. Antimicrobial activity of silver nanoparticles against *E. Coli* U12

In a liquid dilution experiment, the lowest silver nanoparticles concentration that inhibits the visible growth of *E. coli* U12 in liquid medium was 85 $\mu\text{g/ml}$ (MIC). Also, the lowest concentration of silver nanoparticles at which no growth of *E. coli* U12 on solid medium was 127.5 $\mu\text{g/ml}$ (MBC) (Fig. S5).

Using the CFU method, the results revealed that there was a parallel decrease in *E. coli* U12 growth as a function of silver nanoparticles concentration (from 85 to 340 $\mu\text{g/ml}$) during time, increasing up to 7 days compared with the control (Fig. S6).

5.3. Anti-biofilm activity of silver nanoparticles against *E. Coli* U12

In the Congo red agar method, the results showed that all tested silver nanoparticles concentrations completely inhibited *E. coli* U12 biofilm formation. *E. coli* U12 grew as dry, crystalline black colonies in the absence of silver nanoparticles, demonstrating biofilm formation (Fig. S7).

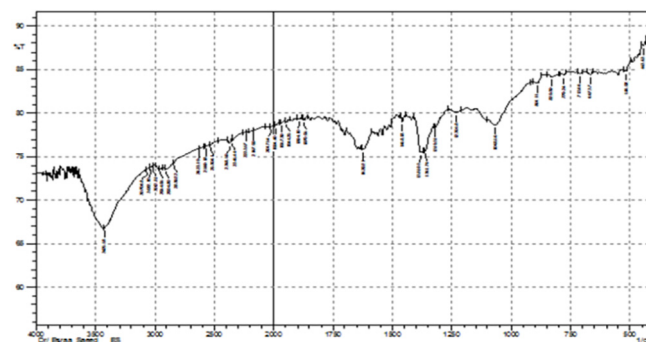


Fig. 1. FTIR Spectroscopic of silver nanoparticles.

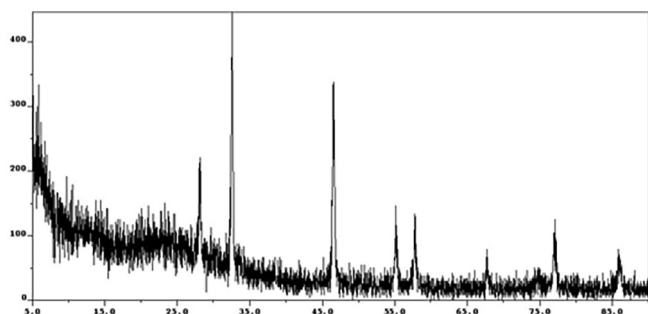


Fig. 2. X-ray diffraction pattern of silver nanoparticles.

In the crystal violet assay method, there was a gradual reduction in the production of biofilm with increasing the concentrations of silver nanoparticles compared with the positive control (Figs. S8 and S9).

5.4. Biofilm production by *E. coli* U12 on a urinary catheter following exposure to silver nanoparticles

In CFU, there was a parallel reduction in *E. coli* U12 adherence to the urinary catheter as a function of silver nanoparticles concentration (from 85 to 340 $\mu\text{g/ml}$) over time, increasing up to seven days compared with the positive control (Fig. S10).

Staining the bounded bacteria on urinary catheter segments with CV indicated that, with increasing the concentration of silver nanoparticles, there was a gradual decrease in the degree of crystal violet stain color that was bound with biofilms on urinary catheters (Fig. S11).

5.5. Scanning and transmission electron microscopy

In SEM analysis, the results demonstrated that *E. coli* U12 adherence to urinary catheter segments was inhibited after treat-

ment with silver nanoparticles concentrations of 85, 255, and 340 $\mu\text{g/ml}$ at 24, 72, and 144 h, respectively, compared with the control (Fig. S12).

In TEM analysis, Fig. (S13) indicated that there was a rupture in the cell wall of *E. coli* U12 cells after exposure to Sub-MIC (42.5 $\mu\text{g/ml}$) of silver nanoparticles for 24 h. Also, some cells undergo partial lysing of their cytoplasmic contents compared with control.

6. Discussion

All of the extract's secondary metabolites are important in the reducing as well as capping mechanisms for nanoparticle synthesis (Marslin et al., 2018). In the present study, silver nanoparticles were produced using *Aloe vera* aqueous extract and had an absorption peak of between 400 and 450 nm.

FTIR is performed as a method of confirmation for nanoparticle production and provides an overview of the rotational and vibrational modes of the compounds that already exist, which aids in the identification of functional and phytochemical compounds that are associated with silver nanoparticles reduction and stability. The broad peaks at 3434 cm^{-1} and 1117 cm^{-1} , respectively, point to the occurrence of OH and C-OH stretching vibrations. According to the FTIR findings, it can be concluded that the presence of proteins, enzymes, and metabolites like carboxylic acid, polyphenols, flavonoids, and alkaloids "that persisted attached to silver nanoparticles following multiple washings" are involved in zinc ion reduction to silver nanoparticles. The existence of free amino as well as carboxylic groups that have bonded to the zinc surface could likely account for the stability of the produced silver nanoparticles. Moreover, the proteins in the medium help to stabilise silver nanoparticles by producing a coat that covers the metal nanoparticles and prevents them from clumping together (Sri Sindhura et al., 2014).

In addition, the (20) peaks angles at 31.77° , 34.42° , 36.26° , 47.54° , 56.60° , 62.86° , 66.38° , 67.95° , 69.09° , 72.57° and 76.97° correlate to the reflection from (100), (002), (101), (102), (110), (103),

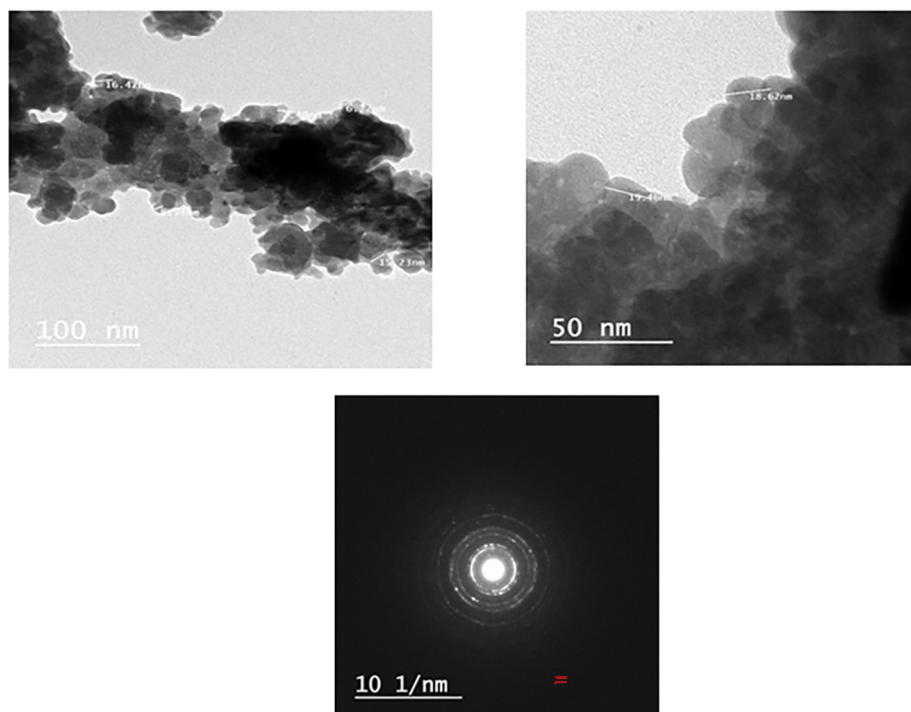


Fig. 3. HR-TEM micrograph of silver nanoparticles.

(200), (112), (201), (004) to (202) crystal planes, respectively according to JCPDS 36–1451 card (John and Rajakumari, 2012). The mean crystallite size of silver was measured to be 15.22 nm utilizing Scherrer's equation, that was determined from the FWHM of the peak that is more intense corresponding to the 101 plane at 36.26°. This lies inside the size range of 9.26 to 31.18 nm, determined via TEM. It has been proven that reducing particle size improves their effectiveness as antibacterial and anticancer agents owing to the high surface-to-volume proportion (Masum et al., 2019).

By decreasing the size of the silver particles to the nanoscale, the antibacterial and anti-biofilm activities of the silver were increased as the surface area of the particles increased. As a result, the level of Ag⁺ release is greater than that of silver particles in their elemental form. Consequently, silver nanoparticles have a better ability to adhere, penetrate, and aggregate inside the cell membrane of bacteria, resulting in a large amount of silver ions being released within the cell. The presence of water channels all over the biofilm could explain silver nanoparticles biofilm inhibitory action. These pores were important in nutrient transport, and silver nanoparticles could pass right through these pores and reveal their antibacterial action (Ansari et al., 2014; Muzammil et al., 2018).

In the present study, different concentrations of silver nanoparticles (85, 127.5, 170, 212.5, 255, 297.5, and 340 µg/ml) were examined for their potential to exhibit antimicrobial effect towards *E. coli* U12 via observing the growth of *E. coli* U12 visually in liquid media and CFU/ml. The results revealed that the MIC and MBC of silver nanoparticles against *E. coli* U12 were 85 µg/ml and 127.5 µg/ml, respectively. The findings revealed that the CFU of *E. coli* U12 proliferation was proportional to silver nanoparticles concentration (from 85 to 340 µg/ml) over time (up to seven days). Our results are in agreement with Rodríguez-Serrano et al. (2020). They discovered that when silver nanoparticles concentration and time increased, the proliferation of uropathogenic *E. coli* was reduced. Skóra et al. (2021) found that silver nanoparticles had a greater antimicrobial activity towards *E. coli*, *S. aureus*, and *P. aeruginosa*.

Regarding the anti-biofilm efficiency, silver nanoparticles were investigated against *E. coli* U12 grown on CRA enriched with and without silver nanoparticles, as well as the CV assay method. When *E. coli* U12 was cultured without silver nanoparticles (control), it developed black, dry crystalline colonies, indicating that exopolysaccharide generation (EPS) is required for biofilm creation. When the uropathogenic *E. coli* U12 was treated with silver nanoparticles, the bacterial growth and production of biofilms were both suppressed at all concentrations. Our findings are consistent with those of Ansari et al. (2014). They found that *E. coli* as well as *K. pneumoniae* treated with silver nanoparticles did not establish biofilm over CRA medium because the generation of glycocalyx matrix and exopolysaccharide synthesis were inhibited. In addition, the current study revealed that when silver nanoparticles concentrations increased, *E. coli* U12 biofilm development in microtitre plate wells decreased gradually. Our findings are similar to those of Ramachandran and Sangeetha (2017). They discovered that rising silver nanoparticles concentrations from 12.5 to 100 µg/ml prevented biofilm development in *Klebsiella pneumoniae*, *Escherichia coli*, as well as *Pseudomonas aeruginosa* within 24 h. Also, Rodríguez-Serrano et al. (2020) showed that silver nanoparticles concentrations ranging from 7.5 to 35 mg/L reduced and impaired the development of biofilms generated by uropathogenic *E. coli* by 97 %.

Also, the present investigation was extended in vitro to control *E. coli* U12 biofilm production on urinary catheter segments. Silver nanoparticles concentrations were investigated for their potential to reduce *E. coli* U12 adherence to urinary catheter segments using

CFU/cm² as well as crystal violet staining of adherent bacteria over urinary catheter segments. The results indicated that the adhesion of *E. coli* U12 to the catheter decreased linearly with a rise in the concentration of silver nanoparticles (from 85 to 340 µg/ml) over time (up to seven days). As the silver nanoparticles concentration increased, the color intensity of the CV stain that was associated with adherent bacteria on the catheter decreased gradually. Our results are compatible with previous published studies that indicated silver nanoparticles biofilm elimination potential is directly correlated with their concentrations. As the concentration of silver nanoparticles increases, the efficiency of biofilm destruction increases (Masák et al., 2014; Thuptimjang et al., 2017). Our findings showed a similar pattern, demonstrating that silver nanoparticles are dose-dependently and can be utilized to treat multidrug-resistant *E. coli* U12. Skóra et al. (2021) found that the efficiency of silver nanoparticles was dose-dependent, with stronger biofilm elimination at concentrations of 1 to 2 µg/mL than at 0.5–0.125 µg/mL doses of silver nanoparticles. Kostenko et al. (2010) showed that silver nanoparticles significantly reduced CFU counts and *Pseudomonas aeruginosa* adhesion. The development of *S. aureus* and *E. coli* biofilms was reduced following long-term exposure to silver nanoparticles. Kumar et al. (2012) found that silver nanoparticles suppressed biofilm development in *E. coli*, *S. aureus*, *Salmonella typhi*, and *Vibrio cholerae*. Ebrahimi et al. (2018) found that silver nanoparticles prevented the biofilm development of *P. aeruginosa*, *A. baumannii*, *E. faecalis*, and *S. aureus* with a 90 % inhibitory activity.

It is very important during the current investigation to confirm the reduction of *E. coli* U12 adhesion following pre-coating of the urinary catheter utilizing silver nanoparticles after SEM inspection. The results revealed that pre-coating with silver nanoparticles lowered the adhesion of *E. coli* U12 as the concentration of silver nanoparticles increased.

Transmission electron microscopy study revealed that silver nanoparticles concentration of 85 µg/ml had a dramatic effect on *E. coli* U12 cells for 24 h. This results in the rupturing of the cell wall and cell membrane, hence the release of the cell contents. Ansari et al. (2014) showed that, after examining biofilms produced by *E. coli* on glass slides for 24 h with SEM, their shape had changed and silver nanoparticles at a concentration of 20 g/ml had an impact on the roughness of the cell surface. Ramachandran and Sangeetha (2017). SEM investigation explained that silver nanoparticles suppressed bacterial growth and exopolysaccharide development by *K. pneumoniae* on glass slides for 24 h. Singh et al. (2021) reported that, after inspection with SEM, the bacterial cells of *P. aeruginosa* and *E. coli* showed changes in morphology with apparent membrane pores, intracellular content leaking, as well as cell lysis after treatment with silver nanoparticles.

7. Conclusion

From these findings, silver nanoparticles have substantial antimicrobial and anti-biofilm activities towards *E. coli* U12. As a result, pre-coating urinary catheters with silver nanoparticles is a good idea and can be widely used in medical applications as anti-biofilm compounds to inhibit and limit the development of bacterial biofilm communities linked to major disorders, including urinary tract infections.

Declaration of Competing Interest

The authors declare that they have no known competing financial interests or personal relationships that could have appeared to influence the work reported in this paper.

Acknowledgments

The authors would like to thank Mansoura University for performing the electron microscope inspection.

Appendix A. Supplementary data

Supplementary data to this article can be found online at <https://doi.org/10.1016/j.sjbs.2022.103457>.

References

- Almalki, M.A., Varghese, R., 2020. Prevalence of catheter associated biofilm producing bacteria and their antibiotic sensitivity pattern. *J. King Saud. Univ. Sci.* 32 (2), 1427–1433.
- Ansari, M.A., Khan, H.M., Khan, A.A., et al., 2014. Antibiofilm efficacy of silver nanoparticles against biofilm of extended spectrum β -lactamase isolates of *Escherichia coli* and *Klebsiella pneumoniae*. *Appl. Nanosci.* 4, 859–868. <https://doi.org/10.1007/s13204-013-0266-1>.
- Bose, S., Khodke, M., Basak, S., Mallick, S.K., 2009. Detection of biofilm producing staphylococci: need of the hour. *J. Clin. Diagn. Res.* 3 (6), 1915–1912.
- Bruna, T., Maldonado-Bravo, F., Jara, P., Caro, N., 2021. Silver Nanoparticles and Their Antibacterial Applications. *Int. J. Mol. Sci.* 22 (13), 7202. <https://doi.org/10.3390/ijms22137202>.
- Camele, I., Elshafie, H.S., Caputo, L., Sakr, S.H., De Feo, V., 2019. *Bacillus mojavensis*: biofilm formation and biochemical investigation of its bioactive metabolites. *J. Biol. Res.* 92 (1).
- Chapman, C.M.C., Gibson, G.R., Todd, S., Rowland, I., 2013. Comparative in vitro inhibition of urinary tract pathogens by single and multi-strain probiotics. *Eur. J. Nutr.* 52 (6), 1669–1677.
- Dytham, C., 1999. *Choosing and Using Statistics: A Biologist's guide*. Blackwell Science Ltd., London UK.
- Ebrahimi, A., Jafferi, H., Habibi, S., Lotfalian, S., 2018. Evaluation of Anti biofilm and Antibiotic Potentiation Activities of Silver Nanoparticles Against some Nosocomial Pathogens. *Iran J. Pharm Sci.* 14 (2), 7–14.
- Ezeonu, I.M., Kanu, J.U., 2016. Inhibition of biofilms on urinary catheters using immobilized *Lactobacillus* cells. *Afr. J. Microbiol. Res.* 10 (25), 920–929.
- Fracchia, L., Cavallo, M., Allegrone, G., Martinotti, M.G., 2010. A *Lactobacillus*-derived biosurfactant inhibits biofilm formation of human pathogenic *Candida albicans* biofilm producers. *Appl. Microbiol. Biotechnol.* 2, 827–837.
- Gudiña, E.J., Teixeira, J.A., Rodrigues, L.R., 2010. Isolation and functional characterization of a biosurfactant produced by *Lactobacillus para casei*. *Colloids Surf. B Biointerfaces* 76 (1), 298–304.
- John, R., Rajakumari, R., 2012. Synthesis and Characterization of Rare Earth Ion Doped Nano ZnO. *Nano-Micro Lett.* 4 (2), 65–72.
- Kostenko, V., Lyczak, J., Turner, K., Martinuzzi, R.J., 2010. Impact of silver-containing wound dressings on bacterial biofilm viability and susceptibility to antibiotics during prolonged treatment. *Antimicrob. Agents Chemother.* 54 (12), 5120–5131.
- Kumar, P., Senthamselvi, S., Lakshmi, P., Premkumar, K., Muthukumar, R., Visvanathan, P., et al., 2012. Efficacy of bio-synthesized silver nanoparticles using *acanthophora spicifera* to encumber biofilm formation. *Dig. J. Nanomater. Biopstruct.* 7 (2), 511–522.
- Li, H., Song, C., Liu, D., Ai, Q., Yu, J., 2015. Molecular analysis of biofilms on the surface of neonatal endotracheal tubes based on 16S rRNA PCR-DGGE and species-specific PCR. *Int. J. Clin. Exp. Med.* 8 (7), 11075–11084.
- Li, X., Sun, L., Zhang, P., Wang, Y., 2021. Novel Approaches to Combat Medical Device-Associated Biofilms. *Coatings* 11 (3), 294. <https://doi.org/10.3390/coatings11030294>.
- Marslin, G., Siram, K., Maqbool, Q., Selvakesavan, R.K., Kruszka, D., Kachlicki, P., Franklin, G., 2018. Secondary Metabolites in the Green Synthesis of Metallic Nanoparticles. *Materials (Basel, Switzerland)* 11 (6), 940. <https://doi.org/10.3390/ma11060940>.
- Masák, J., Čejková, A., Schreiberová, O., Rezanka, T., 2014. *Pseudomonas* biofilms: possibilities of their control. *FEMS Microbiol. Ecol.* 89 (1), 1–14.
- Masum, M., Siddiqi, M.M., Ali, K.A., Zhang, Y., Abdallah, Y., Ibrahim, E., Qiu, W., Yan, C., Li, B., 2019. Biogenic Synthesis of Silver Nanoparticles Using *Phyllanthus emblica* Fruit Extract and Its Inhibitory Action Against the Pathogen *Acidovorax oryzae* Strain RS-2 of Rice Bacterial Brown Stripe. *Front. Microbiol.* 10, 820. <https://doi.org/10.3389/fmicb.2019.00820>.
- Mekky, A.F., Hassanein, W.A., Reda, F.M., Elsayed, H.M., 2022. Anti-biofilm potential of *Lactobacillus plantarum* Y3 culture and its cell-free supernatant against multidrug-resistant uropathogen *Escherichia coli* U12. *SJBS* 29 (4), 2989–2997.
- Mirzajani, F., Ghassempour, A., Aliahmadi, A., Esmaeili, M.A., 2011. Antibacterial effect of silver nanoparticles on *Staphylococcus aureus*. *Res. Microbiol.* 162 (5), 542–549.
- Muhammad, M.H., Idris, A.L., Fan, X., Guo, Y., Yu, Y., Jin, X., Qiu, J., Guan, X., Huang, T., 2020. Beyond Risk: Bacterial Biofilms and Their Regulating Approaches. *Front. Microbiol.* 11, 928. <https://doi.org/10.3389/fmicb.2020.00928>.
- Muzammil, S., Hayat, S., Fakhar-E-alam, M., Aslam, B., Siddique, M.H., Nisar, M.A., Saqalein, M., Atif, M., Sarwar, A., Khurshid, A., Amin, N., Wang, Z., 2018. Nanoantibiotics: Future nanotechnologies to combat antibiotic resistance. *Front. Biosci. (Elite edition)* 10, 352–374.
- Parvekar, P., Palaskar, J., Metgud, S., Maria, R., Dutta, S., 2020. The minimum inhibitory concentration (MIC) and minimum bactericidal concentration (MBC) of silver nanoparticles against *Staphylococcus aureus*. *Biomater. Investig. Dent.* 7 (1), 105–109.
- Patra, J.K., Das, G., Fraceto, L.F., Campos, E., Rodriguez-Torres, M., Acosta-Torres, L.S., Diaz-Torres, L.A., Grillo, R., Swamy, M.K., Sharma, S., Habtemariam, S., Shin, H.S., 2018. Nano based drug delivery systems: recent developments and future prospects. *J. Nanobiotechnol.* 16 (1), 71. <https://doi.org/10.1186/s12951-018-0392-8>.
- Ramachandran, R., Sangeetha, D., 2017. Antibiofilm efficacy of silver nanoparticles against biofilm forming multidrug resistant clinical isolates. *J. Pharm. Innov.* 6, 36–43.
- Rodríguez-Serrano, C., Guzmán-Moreno, J., Ángeles-Chávez, C., Rodríguez-González, V., Ortega-Sigala, J.J., Ramírez-Santoyo, R.M., Vidales-Rodríguez, L.E., Mishra, Y. K., 2020. Biosynthesis of silver nanoparticles by *Fusarium scirpi* and its potential as antimicrobial agent against uropathogenic *Escherichia coli* biofilms. *PLoS One* 15 (3), e0230275.
- Rosenthal, V.D. et al., 2012. International Nosocomial Infection Control Consortium report, data summary of 36 countries, for 2004–2009. *Am. J. Infect. Control* 40 (5), 396–407.
- Roy, R., Tiwari, M., Donelli, G., Tiwari, V., 2018. Strategies for combating bacterial biofilms: A focus on anti-biofilm agents and their mechanisms of action. *Virulence* 9 (1), 522–554.
- Shaikh, S., Nazam, N., Rizvi, S., Ahmad, K., Baig, M.H., Lee, E.J., Choi, I., 2019. Mechanistic Insights into the Antimicrobial Actions of Metallic Nanoparticles and Their Implications for Multidrug Resistance. *Int. J. Mol. Sci.* 20 (10), 2468. <https://doi.org/10.3390/ijms20102468>.
- Singh, P., Pandit, S., Jers, C., Joshi, A.S., Garnæs, J., Mijakovic, I., 2021. Silver nanoparticles produced from *Cedecea* sp. exhibit antibiofilm activity and remarkable stability. *Sci. Rep.* 11, 12619. <https://doi.org/10.1038/s41598-021-92006-4>.
- Skóra, B., Krajewska, U., Nowak, A., Dziedzic, A., Barylyak, A., Kus-Liśkiewicz, M., 2021. Noncytotoxic silver nanoparticles as a new antimicrobial strategy. *Sci. Rep.* 11 (1), 13451. <https://doi.org/10.1038/s41598-021-92812-w>.
- Sri Sindhura, K., Prasad, T.N.V.K.V., Selvam, P., Hussain, O.M., 2014. Synthesis, characterization and evaluation of effect of phytochemical zinc nanoparticles on soil exo-enzymes. *Appl. Nanosci.* 4, 819–827. <https://doi.org/10.1007/s13204-013-0263-4>.
- Thuptimrang, P., Limpiyakorn, T., Khan, E., 2017. Dependence of toxicity of silver nanoparticles on *Pseudomonas putida* biofilm structure. *Chemosphere* 188, 199–207.
- Tippayawat, P., Phromviyo, N., Boueroy, P., Chompoosor, A., 2016. Green synthesis of silver nanoparticles in aloe vera plant extract prepared by a hydrothermal method and their synergistic antibacterial activity. *Peer J.* 4, e2589.

Further Reading

- Goldstein, F.W., Dang Van, A., Bouanchaud, D.H., Acar, J.F., 1988. Evolution de la resistance aux antibiotiques de pneumocoques et repartition de leurs types capsulaires. *Pathol. Biol.* 15, 126–173.